PAPER

Flumequine-loaded titanate nanotubes as antibacterial agents for aquaculture farms

Tarek Baati, [ID] *[a] Mounir Ben Brahim,[a] Abir Salek,[a] Mouna Selmi,[a] Leila Njim,[b] Polona Umek, [ID] [c] Aicha Aouane,[d] Mohamed Hammami [ID] [a] and Karim Hosni[a]

Flumequine (FLUM), a quinolone-derived antibiotic is one of the most prescribed drugs in aquaculture farms. However, its intensive use becomes worrisome because of its environmental risks and the emergence of FLUM-resistant bacteria. To overcome these problems we propose in this study the encapsulation and the delivery of FLUM by titanate nanotubes (TiNTs). Optimal FLUM loading was reached by suspending the dehydrated powder nanomaterials (FLUM : TiNTs ratio = 1 : 5) in ethanol. The drug entrapment efficiency was calculated to be 80% approximately with a sustained release in PBS at 37 °C up to 5 days. Then FLUM@TiNTs was evaluated for both its *in vitro* drug release and antimicrobial activity against *Escherichia coli* (*E. coli*). Spectacularly high antibacterial activity compared to those of free FLUM antibiotic was obtained confirming the efficiency of TiNTs to protect FLUM from rapid degradation and transformation within bacteria improving thereby its antibacterial effect. Indeed FLUM@TiNTs was efficient to decrease gradually the bacterial viability to reach ≈5% after 5 days *versus* ≈75% with free FLUM. Finally, the *ex vivo* permeation experiments on sea bass (*Dicentrachus labrax*) intestine shows that TiNTs act to increase the intestinal permeation of FLUM during the experiment. Indeed the encapsulated FLUM flux increased 12 fold (1.46 μg cm^2 h^{-1}) compared to the free antibiotic (0.18 μg cm^2 h^{-1}). Thanks to its physical properties (diameter 10 nm, tubular shape…) and its high stability in the simulated intestinal medium, TiNTs are easy internalized by enterocytes, thus involving an endocytosis mechanism, and then improve intestinal permeation of FLUM. Taken together, FLUM@TiNTs hold potential as an effective approach for enhancing the antimicrobial activity of FLUM and pave the way not only for future pharmacokinetic studies in the treatment and targeting of fish infections but also for instating of novel strategies that overcome the challenges associated with the abusive use of antibiotics in fish farming.

1 Introduction

With the expansion of marine ranching and the fish farming industry, demand for antibiotics has dramatically increased during the lasts decades, and the projected worldwide use of antibiotics in livestock is estimated to be 106 000 tons in 2030.[1,2] Antibiotics are usually given to fish as medicated feed. As an immediate consequence of the oral administration, a large part of the antibiotics (70 to 80%) ends up in the aquatic environment, either directly because the molecules diffuse into the water from the unconsumed food, or indirectly because the molecules are weakly absorbed, and then excreted in urine and feces.[3,4] As a consequence of the excessive use of antibiotics in aquaculture, antibiotic resistance is induced in the surrounding bacteria in the sediment and fish-associated bacterial strains. One of the most frequently used antibiotics in aquaculture farming is the flumequine (FLUM) which is a broad-spectrum synthetic antibacterial agent of the quinolones class. FLUM has an antimicrobial activity against Gram-negative microorganisms.[5] It is administered orally to various animal species for treatment of enteric infections.[6] Several works reported the problem of the fast absorption and excretion of FLUM from plasma and tissues of different fish species such as lumpfish,[7] Atlantic salmon,[8,9] turbot[10] and Atlantic halibut,[11] thus inducing considerable variation in plasma concentration.[12] FLUM has an adequate kinetic profile in gilthead sea bream but marine cations induce a significant impact on its activity rendering its use against bacterial pathogens questionable.[13] Alternative strategies to improve absorption rates of antibiotics and reducing their release in the aquatic environment are of primary interest. Recently, the use of nanoparticles/nanomaterials as efficient antibiotics delivery systems has received particular attention. The commonly studied nanosystems for antibiotic loading are inorganic metal, silica,

[a]Laboratoire des Substances Naturelles, Institut National de Recherche et d'Analyse Physico-chimique, Biotechpôle Sidi Thabet, 2020 Tunisia. E-mail: tarek.baati@gmail.com; Tel: +216 71 537 666

[b]Service d'Anatomie Pathologique, CHU de Monastir, Université de Monastir, Tunisia

[c]Jožef Stefan Institute, Jamova cesta 39, SI-1000 Ljubljana, Slovenia

[d]Centre de Microscopie Electronique, IBDML campus Luminy Marseille, 13000, France

polymeric, lipid-based, and micellar nanoparticles.[14] The main problem limiting the use of metallic nanoparticles, especially Si, carbon, Au-, Ag-, or Cu-based nanoparticles is their potential cellular toxicity.[15] Concerning the polymeric, lipid-based, and micellar nanoparticles, their instability *in vivo* is one of the principal disadvantages which limited their use for drug delivery.[16] Titanate nanotubes (TiNTs) stand out among inorganic nanomaterials for their tubular shape, leading to a higher cellular internalization, high surface and large pore volume conferring higher drug loading capacity.[17,18] The use of TiNTs as nanocarriers for drug delivery has already been reported.[19,20] In our previous works, we have studied the capacity of TiNTs for genistein loading and its antitumor activity on U87-MG line cells. We have demonstrated that TiNTs could achieve higher genistein drug-loading content (25.2%) and entrapment efficiency (51.2%) leading to a controlled drug release as well as a higher cellular uptake of genistein-loaded-TiNTs.[21] No debate on the biocompatibility of TiNTs since their safety was confirmed on mice either after 45 days of the intravenous administration of a relatively high dose (45 mg kg^{-1}).[22] Nevertheless, a nanoantibiotics with preserved antibacterial efficacy has recently been synthesized by self-assembly of FLUM on iron oxide nanoparticles.[23] However several chemical process were needed to produce stable nanocarriers such binding of the organic molecule to nanoparticles by the chelation of under-coordinated Fe^{3+} sites on magnetic nanoparticles surface and by the reactivity of carboxyl functionality of the antibiotic. Unfortunately these reactions are costly and needs time. Likewise no information about the capacity of these nanoparticles to load FLUM and their stability for a long time, were reported. Since TiNTs are biologically and chemically inert, inexpensive, nontoxic and stable in both water and biological medium, we aimed in this work the development of these nanomaterials as a novel nanocarrier for FLUM for aquaculture application. Firstly we studied the stability of TiNTs in Ringer solution (simulated intestinal medium) and Mueller Hinton broth then their loading capacity of FLUM and the release kinetics. The secondary purpose was to study the antibacterial effect of FLUM@TiNTs on *Escherichia coli* (*E. coli*) and its intestinal permeation in the Ussing chamber using sea bass intestine as a model of aquaculture species. The bacterial strain is not only selected for its omnipresence in aquatic environments, but also, as an excellent model microorganism for studying the ecotoxicity of nanoparticles and the cell organism–nanoparticles interaction.[24] It is expected that FLUM@TiNTs formulation improve significantly the antibiotic tissues and cells uptake then targeting fish infections. Thanks to high capacity of drug loading with an effective sustained release, TiNTs can reducing the excessive use of antibiotic, and consequently decontaminate the polluted environment.

2 Materials and methods

2.1. TiNTs synthesis and characterization

TiNTs were prepared by a classical hydrothermal method and characterized as reported previously.[18] Surface charge was determined by Malvern Zetasizer 2000 (Zetasizer Nano ZS90,

Malvern Instruments Ltd, UK). Before measurement, the freshly prepared TiNTs were appropriately suspended in pure water (0.1 mg mL^{-1}) then ultrasonicated during 5 min. Then a sample of TiNTs suspension was observed by TEM using transmission electron microscope Tecnai G2 at 200 kV (FEI, Netherland) and acquire with a Veleta camera (Olympus, Japan). For crystalline phase X-ray powder diffraction was performed at room temperature with an X-ray diffractometer (X' Pert PRO MPD, PANalytical Co., Holland). Monochromatic Cu Kα-radiation ($\lambda = 1.5418$ Å) was obtained with a Ni-filtration and a system of diverging and receiving slides of 0.5° and 0.1 mm respectively. The diffraction pattern was measured with a voltage of 40 kV and a current of 30 mA over a 2θ range of 3–40° using a step size of 0.02° at a scan speed of 1 s per step.

2.2 TiNTs stability study

Stability studies were performed by suspending 1 mg of TiNTs in 100 mL of Mueller Hinton broth (M–H broth) or Ringer media (simulated intestinal media at pH = 6.0). The suspensions were stirred under bidimensional continuous stirring in an incubator at 60 × 60 rpm at 37 °C for 7 days. In order to recover the nanotubes and liquid phases, the suspensions were centrifuged at 14 500 rpm during 15 minutes. The pellet was washed with fresh ultra pure water and analyzed by XRD (X-ray diffraction) for crystallinity then the Ti released in the supernatant was determined by ICP-MS as reported previously.[20]

2.3 Drug loading and entrapment efficiency

TiNTs powder was dehydrated at 70 °C for 16 hours in order to remove water and residual solvent into the pores. Three concentration of TiNTs 5 mg mL^{-1}, 10 mg mL^{-1} and 20 mg mL^{-1}, were tested for FLUM entrapment by suspending the nanotubes powder in 5 mL of ethanol FLUM solution (1 mg mL^{-1}) at room temperature under continuous magnetic stirring during 24 hours. Different samples were prepared in triplicate for each entrapment time (0.5 h, 1 h, 3 h, 6 h, 8 h and 24 h). Then samples were centrifuged for 15 min at 14 000 rpm in order to recover separately the nanotubes and the supernatant. The TiNTs entrapped FLUM amount was determined by thermogravimetric analysis (TGA) and High Performance Liquid Chromatography (HPLC) in the nanomaterials and the supernatant respectively. Additionally, TiNTs before and after the FlUM entrapping were characterized by X-ray powder diffraction (XPRD), TEM and finally the FITR spectra have been performed.

2.4 *In vitro* drug release

FLUM release was carried out in triplicate by soaking 5 mg of antibiotic-loaded-TiNTs in 20 mL of phosphate buffer solution (PBS 0.04 M, pH 7.4) at 37 °C under a continuous bidimensional stirring (120 rpm; incubator Multitron Ortibale 50 mm, HT Infors, France). In order to determine the kinetic of FLUM release, 16 samples of 1 mL were recovered from supernatant, obtained after centrifugation 14 500 rpm for 15 min, from 5 min post stirring up to 7 days. Samples are recovered and replaced with the same volume of fresh medium at 37 °C.

The drug concentration was then determined in the supernatants by HPLC.

2.5 Fourier transforms infrared spectroscopy (FTIR) analysis

FTIR spectra were recorded to confirm the chemical structures of FLUM and TiNTs and to evaluate any probable drug/carrier interaction in the prepared formulation. Small amounts of materials were analyzed using a Thermo Nicolet spectrometer (Thermo, USA). The spectra were recorded from 4000–400 cm^{-1}.

2.6 Thermogravimetric analysis (TGA)

After 12 h of FLUM encapsulation samples were centrifuged at 14 000 rpm to recover the FLUM loaded nanomaterials (FLUM@TiNTs). For TGA measurements TiNTs or FLUM@-TiNTs samples (5 mg) were analyzed under an oxygen flow (20 mL min^{-1}) using a PerkinElmer Diamond TGA/DTA STA 6000 running from room temperature (25 °C) to 800 °C with a scan rate of 10 °C min^{-1}. Typically, FLUM containing samples show two different weight losses. The first weight loss, between 30 and 150 °C, is due to the departure of water, the second one more differentiated (from around 200 to 300 °C) corresponds to the FLUM departure. The amount of FLUM was estimated considering the weight losses of the empty and dried TiNTs (mg of FLUM per 100 mg of dry TiNTs).

2.7 Antibacterial activity

Experiments were performed using the *Escherichia coli* (*E. coli*, ATCC 25922™) which represent a recommended reference strain for antibiotic susceptibility testing. Freeze-dried cells were activated according to the National committee for clinical laboratory standards (NCCLS) guidelines.[25] Each strain was maintained on a nutrient agar slant. The stock cultures were transferred to 100 mL of Mueller Hinton broth and were grown in an air bath incubator with a reciprocal shaker for 24 h at 150 rpm and 37 °C until stationary phase. Bacterial cultures were centrifuged at 3000 rpm for 15 min then washed twice with 0.9% physiology salt solution. The bacterium suspensions (100 mL) were prepared by resuspending the bacterial pellets in Mueller Hinton broth with the cell concentration determined by the turbidity absorbance at 600 nm as recommended by the Clinical and Laboratory Standards Institute guidelines.[26] The bacterial culture suspensions were adjusted at 0.5 McFarland turbidity by different dilution to obtain grown at exponential phase which correspond to 10^6 CFU per mL. In order to study the antibacterial activity of FLUM@TiNTs on *E. coli* growth, 1 mL of TiNTs or FLUM@TiNTs (100 μg mL^{-1}) or its equivalent of free FLUM (8 μg mL^{-1}) were added into the bacterial suspension. Then the culture turbidity was continuously monitored photometrically at 6 h, 1, 2, 3, 4, 5 and 7 days post incubation. All treatments including the control were repeated in triplicate.

2.8 Transmission electron microscopy (TEM) analysis

E. coli cells were centrifuged at 3000 rpm for 10 min at 4 °C. After removing of the supernatant, the bacterial pellet was washed twice with a NaCl solution (0.9%) then fixed with 2.5% glutaraldehyde (TAAB) for more than 4 h following a wash step of three time with phosphate buffer (0.1 M; pH 7.0) for 15 min. The cells were post-fixed with 1% OsO$_4$ for 1 to 2 h and were again washed three times with phosphate buffer (0.1 M; pH 7.0) for 15 min. Next, the samples were dehydrated by a graded ethanol series and were then transferred to absolute acetone. The dehydrated samples were embedded in Spur's resin, incubated for 4 h at room temperature, and then placed in an oven (65 °C) for 24 h to polymerize. Finally sections of 90 nm were prepared with a diatom diamond knife on an LBK ultramicrotom Leica UCT and stained with 0.5% aqueous uranyl acetate followed by Reynold's lead citrate. The observation was done with a Tecnai G2 at 200 kV (FEI, Netherland) and acquire with a Veleta camera (Olympus, Japan).

2.9 Intestinal permeation

2.9.1 Animals. All the procedures involving animals are in compliance with the care and use guidelines of experimental animals established by the Ministry of Higher Education and scientific research of Tunisia, and the study was approved by the ethics committee of Monastir University. Moreover, this experiment was directed by accredited scientists (following FELASA category C recommendations) and conducted according to the European Union Directive (2010/63/EU) on the protection of animals for scientific purposes. Specimens of sea bass (*Dicentrachus labrax*) of 100–150 g farmed at the aquaculture farm of Ruspina fish (Monastir, Tunisia) were used. 16 fishes were acclimated for 15 days to laboratory conditions in a 1000 L aquarium filled with clean seawater maintained constantly at 16 °C. Food was automatically distributed daily with extruded pellet for marine fish. Twenty four hours before intestine collection, animals were fasted.

2.9.2 Preparation of the intestinal tissue. The whole intestine of fishes was carefully removed and washed twice with chilled physiological saline solution (NaCl 0.9%). Intestine was excised and cut into segments of 2–3 cm length. After visual examination of the tissue, sections containing Peyer's patches were discarded from the studies.[27] Intestine portions were opened along the mesenteric border and carefully mounted in the Ussing chambers.

2.9.3 Permeation assay. The permeation Ussing chambers consist of two compartments containing Ringer media (acceptor and donor) separated by intestine membrane. During all the experiment, both compartments were oxygenated and circulated by bubbling with carbogen (95% O$_2$/5% CO$_2$), keeping the temperature at 37 °C. The bubbling of the solutions is an essential factor for the viability of the intestinal membranes, but also to avoid the sedimentation of the nanomaterials. The intestinal segment was placed into the diffusion chambers in the inner area of the intestine (intestinal mucosa) faced to the donor compartment and serosa to the receptor one, leaving an available diffusion area of 1 cm^2 then were stabilized during 1 h. Moreover the tissue viability and integrity were controlled by monitoring the transepithelial electrical resistance (TEER) using a potentiometer and the pH values of the

donor and receptor compartments.[28]. FLUM (8 µg mL^{-1}), TiNTs (100 µg mL^{-1}) or FLUM@TiNTs (100 µg mL^{-1}) were suspended in the donor compartment. Permeating studies were performed for 2 h at 37 °C. The intestinal permeation was monitored by collecting several aliquots (1 mL) from the receptor compartment at different times (0.5, 1, 1.5 and 2 h) and replaced with the same volume of fresh medium pre-equilibrated at the experimental temperature conditions (37 °C). At the end of each experiment, the collected aliquots were analyzed by HPLC and ICP-AES in order to quantify the intestinal crossing of FLUM and TiNTs respectively. All the experiments were performed by triplicate for each experimental data. The intestinal diffusion flux (µg cm^{-2} h^{-1}) was calculated by using the equation $F = (dQ/dt)/A$, where dQ/dt (µg h^{-1}) represents the permeability rate, and A (cm^2) is the effective surface area of the intestinal mucosa which is equal to 1 cm^2.[29] Moreover, the permeability coefficient (P, cm h^{-1}) was calculated by using the equation $P = F/Q$, where Q (µg mL^{-1}) is the initial concentration of the studied compound in the donor chamber. Subsequently, the viability of the intestinal membrane was studied by measuring the conductivity (I_{sc}, µA cm^{-2}) of the membrane through the modulation of the ion channels. Firstly, 50 µL of forskolin were added to the donor media in order to open the ion channels, as forskolin-induced K channel activities.[29,30] After 10 minutes, 50 µL of bumetanide were added in order to restart the normal membrane conditions.[31]

2.9.4 Histological analysis. For histological evaluation, intestine segments were fixed in 5% buffered neutral formalin and embedded in a paraffin wax. Sections of 5 µm were cut from each block, and stained primarily with hematoxylin and eosin (H&E) for histopathological study as described previously.[25]

2.10 Flumequine determination by HPLC

FLUM concentration was determined by high-performance liquid chromatography (HPLC) analytical method as described previously.[32] After samples centrifugation at 14 000 rpm for 15 min, 0.5 mL of the supernatant were diluted (v/v) in mobile phase of methanol–0.1 M phosphate buffer, pH 3 (45 : 55, v/v) and added to a quinaldic acid (10 µg mL^{-1} in methanol) sample used as internal standard for error determination. Then after filtration in 0.2 µm porosity filter 20 µL of the sample were injected in the chromatograph. FLUM concentration was determined by reversed-phase HPLC using Sunfire C18 column (3.5 µm, 4.6 × 150 mm) and UV detector coupled to photodiode array (PDA) with detection at 254 nm. A standard calibration curve was obtained after HPLC analysis of FLUM standards prepared in methanol at concentrations ranging from 0.1 µg mL^{-1} to 10 µg mL^{-1}.

2.11 Statistics

Data are shown as the mean ± standard deviation. Comparisons with control were performed for quantitative variable by using Tukey HSD test and SPSS 12 software. A value of $p < 0.05$ was considered statistically significant.

3 Results

3.1 TiNTs characterization

The TEM image from Fig. 1A shows the surface morphology of TiNTs corresponding to elongated tunable tubes with length ranging between 80 nm and 1 µm. Transmission electron microscopy analysis (Fig. 1C, yellow arrow) shows the typical morphology of multi-walled nanotubes with size of 8–10 nm in outer diameter and 4 nm in inner diameter. All the nanotubes were open at both ends. Interestingly, FLUM entrapment increases the zeta potential value from −35 mV in empty TiNTs to −22 mV in FLUM@TiNTs. Crystalline phase of TiNTs before and after FLUM encapsulation, was checked by XRD, confirming not only that the impregnation step does not alter their crystalline structure, but also, in accordance with a significant change in the Bragg peaks relative intensity, the filling of the pores by FLUM molecules (Fig. 1G).

3.2 TiNTs stability study

The stability of TiNTs was studied at 37 °C in both Ringer solution and M–H broth under continuous stirring up to 7 days. As shown in (Fig. 2A), no morphological changes in the TiNTs crystalline structure were observed as confirmed by XRD. Moreover the level of Ti (%) released from degraded nanotubes in Ringer solution (0.18% ± 0.072) and M–H broth (0.22% ± 0.053) was very low during 7 days showing that TiNTs are highly stable in both medium.

3.3 Flumequine loading TiNTs and entrapment efficiency

FLUM loading was carried out by a simple impregnation method by suspending the milled TiNTs powder at different concentrations into ethanol FLUM solutions (1 mg mL^{-1}) for 24 h. The lower concentration of TiNTs (5 mg mL^{-1}) was inefficient to achieve satisfactory drug loading (data not shown). Likewise an important inaccuracy in the FLUM payload estimation occurs with the higher concentration of TiNTs (20 mg mL^{-1}) probably due to the imbalance between the amounts of drug and nanotubes which rules out such encapsulation tests (data not shown). Optimal FLUM loading was reached by suspending the dehydrated powder nanomaterials (FLUM : TiNTs ratio = 1 : 5) equivalent to 10 mg mL^{-1} of TiNTs and 1 mg L^{-1} of FLUM. Indeed a high entrapment efficiency of FLUM up to 80% (±3.12%) was achieved after 8 h of encapsulation (Fig. 1D). Additionally, the amount of the encapsulated FLUM remained unchanged after 8 h of entrapment suggesting a saturation of the pores of multilayer TiNTs. Further, TGA measurement was carried out to confirm this result (Fig. 1F). Indeed different weight losses were observed in the thermogram of FLUM@TiNTs; the first weight loss between 50 and 150 °C due to the departure of water and ethanol, then a second one more differentiated (from 200 to 300 °C) which correspond to the FLUM departure. The amount of FLUM was estimated considering the weight losses of the mg of FLUM per 100 mg of dry TiNTs which is 78 wt% approximately. Concerning the empty nanotubes, the single stage weight loss of roughly 10% observed around 120 °C is ascribed to the release of physisorbed
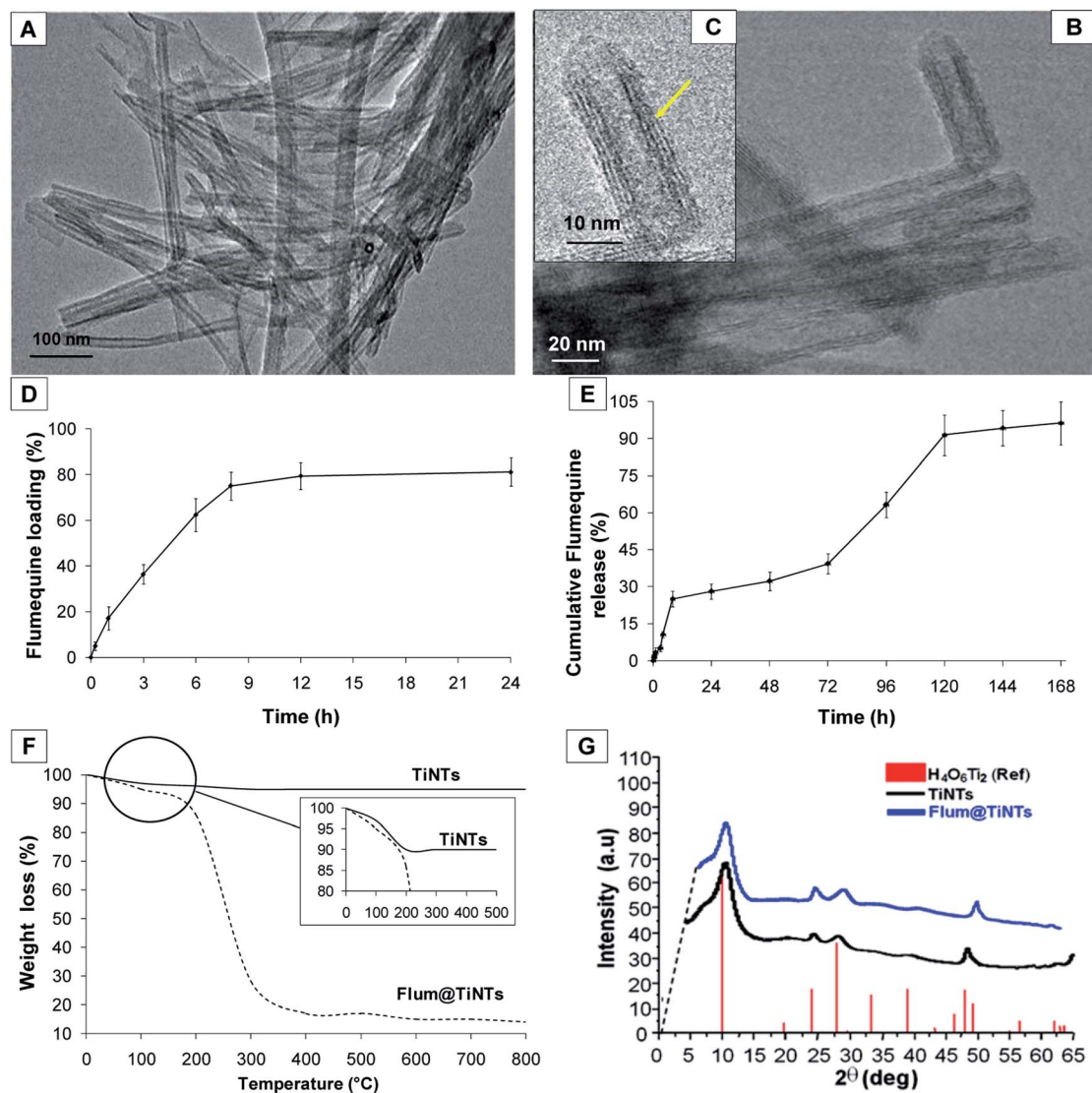
Fig. 1 Characterization of titanate nanotubes (TiNTs) and analysis of flumequine (FLUM) loading. (A–C) TEM images of (TiNTs), (C) magnification of (B) showing the multiple rolled layers of TiNTs (yellow arrow). (D) Kinetic of FLUM TiNTs loading. (E) Cumulative release of FLUM in PBS at 37 °C under continuous stirring. All experiments were carried out in triplicate ($n = 3$). (F) TGA measurement of empty TiNTs samples and FLUM@TiNTs. The magnification shows the weight loss of TiNTs between 100 and 200 °C. (G) XRD pattern of empty TiNTs and FLUM@TiNTs compared to the standard diffractogram of $H_4O_6Ti_2$.

water molecules onto the surface and into the pores. A weak endothermic peak occurred at around 170 °C may be due to chemisorbed and structural water losses including hydroxyl groups of Ti–OH bonds within the tubular architecture. At the end, the kinetics at which FLUM is entrapped within TiNTs is another interesting point to be addressed. Indeed TiNTs showed a fast kinetics of encapsulation, with, for instance, FLUM loading approximately 20% after 3 h of the immersion. Then 8 h post immersion FLUM loading % remains unchanged consistent with a relatively high drug–TiNTs affinity. Concerning the FLUM release profile (Fig. 1E), it was firstly consisting with a burst release of 5% of the total content in a short time, 3 h following the shaking of FLUM@TiNTs in the PBS at 37 °C. Then the cumulative release of FLUM increases slowly and linearly to achieve more than 90% after 5 days. Note that the

percentage of drug release remained unchanged 6 and 7 days following shaking; it achieved more than 95% (±6.2%) of the drug total content showing the total release of FLUM from TiNTs.

3.4 FTIR analysis

The FITR spectrum of FLUM@TiNTs present several new peak compared to that of TiNTS indicating the entrapment of FLUM inside TiNTs (Fig. 3). Indeed in the FLUM@TiNTs FT-IR spectrum, a peak at 1050 cm^{-1} was assigned to C–F group as reported previously.[33] The peaks at 1230 and 1455 cm^{-1} were related to C–O. A band at 3016 cm^{-1} indicated alkenes and aromatic C–H stretching.[22] Another two attached sharp peaks were observed at 1735 cm^{-1} and 1625 cm^{-1}; those can be
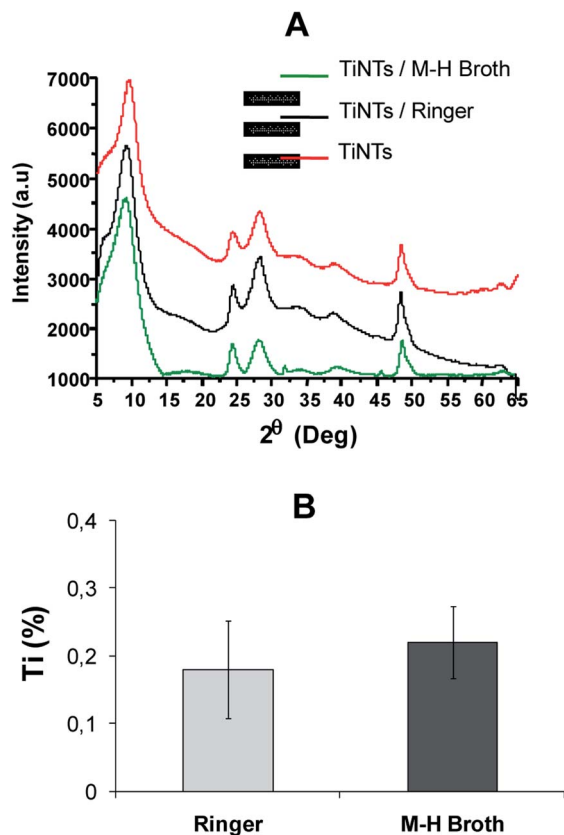
Fig. 2   (A) XRD pattern of TiNTs after 7 days of incubation at 37 °C in M–H broth or in the Ringer solution (simulated intestinal medium) compared with XRD pattern of non incubated nanotubes showing no morphological changes in the TiNTs crystalline structure. (B) The percentage (%) of TiNTs degradation in both Ringer solution and M–H Broth calculated *via* Ti concentration determined after 7 days of incubation at 37 °C under continuous stirring. Results are representative of three independent experiences. No significant differences were observed as confirmed by statistical Tukey HSD test.
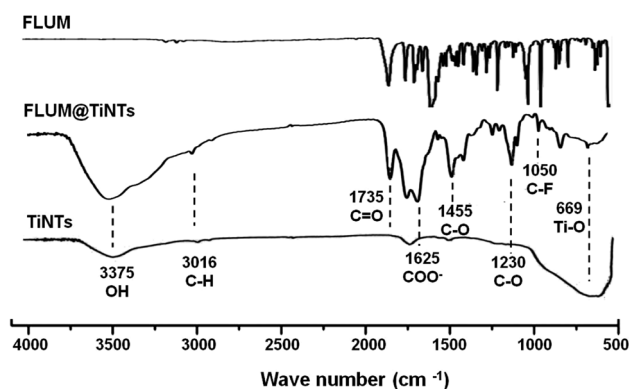

Fig. 3   FTIR spectra of flumequine (FLUM), titanate nanotubes (TiNTs) and flumequine-loading TiNTs (FLUM@TiNTs).

attributed to stretching vibration of C=O present in carboxylic and/or carbonyl moiety groups. A characteristic band at 3375 cm^{-1} present in both TiNTs and FLUM@TiNTs FT-IR spectrum was related to the OH stretching vibration.[34]

3.5   Antibacterial activity

Antibacterial activity was evaluated by monitoring the *E. coli* growth in the presence of TiNTs or FLUM@TiNTs (100 μg mL^{-1}) or its equivalent of free FLUM (8 μg mL^{-1}). The growth curve of *E. coli* in the presence of TiNTs (Fig. 4) is similar to that of the control without any significant statistical differences and clearly depicted an exponential phase characterized by an increased turbidity (OD ≈ 4.78 after 5 days incubation). In the presence of FLUM@TiNTs, the exponential phase was achieved from 6 h to 24 h, and then decreased gradually to reach ≈5% of bacterial viability at the end of experiment (5 days). In contrast, exposed to free FLUM, the bacterial growth is significantly decreased from 6 h (OD = 0.2) until 72 h thereafter increases progressively to achieve an OD of 3.4 at 5 days corresponding to 75% of bacterial viability.

Finally, the morphological changes of the bacterial cells were examined by TEM. In the absence or presence of nanotubes, the bacterial cells presented a normal morphological aspect with characteristic circular shapes and well defined cell walls high electron density forms (Fig. 5). Moreover, TiNTs were observed as aggregates of condensed materials (red arrows) not only in the growth microbial solution but also inside cytoplasm without inducing any cytotoxic effect. In contrast, TEM images of FLUM-treated *E. coli* show serious bacterial cell damage including extended vacuolization (around 100 nm, Fig. 5 asterisk), cell membrane disruption, and leakage of cytoplasmic materials (black arrow). Treatment with FLUM@TiNTs resulted in acute cytotoxicity with severe damage as revealed by the presence of fragmented membrane as well as pits and gaps in bacterial cells membranes. Concomitantly, cells with irregular shape, reduced size and clear cytoplasm were observed in the presence of FLUM@TiNTs which were easily distinguished as aggregates of condensed materials (red arrows). Aggregates of FLUM@TiNTs were tightly attached to the bacterial cells surface prior membrane absorption inside bacteria cytoplasm (yellow circle).
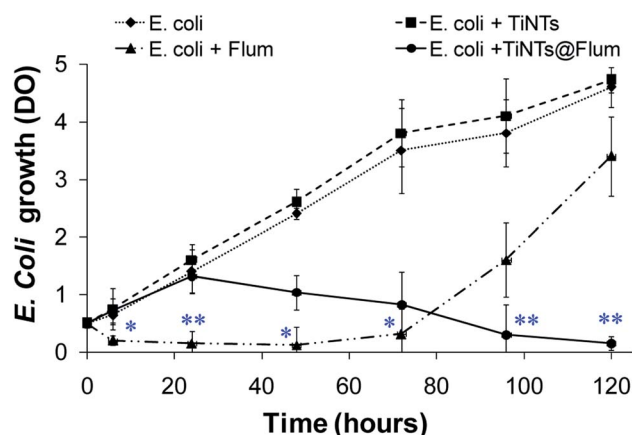

Fig. 4   *E. coli* growths determined by optic density (OD) at 600 nm during 5 days after incubation with 100 μg mL^{-1} of TiNTs or FLUM@TiNTs or its equivalent of free FLUM 8 μg mL^{-1}. Results are representative from three independent experiments (means ± SD, $n = 3$). Statistical significance was determined by Tukey HSD test (*$p < 0.05$, **$p < 0.01$).
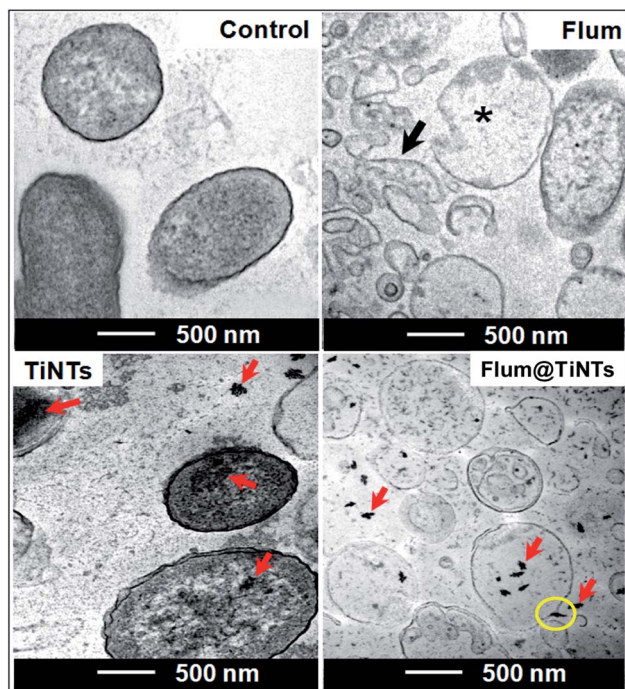
Fig. 5 TEM images of control and treated *E. coli* for 72 h with 100 μg mL^{-1} of titanate nanotubes (TiNTs) or 8 μg mL^{-1} of flumequine (FLUM) or 100 μg mL^{-1} of FLUM@TiNTs.

3.6 Intestinal permeation

Prior to the permeation analysis, the viability of intestine membrane was checked during and at the end of the experiment with regards to the electrical parameters particularly the transepithelial electrical resistance. The TEER recording for the control intestine and those exposed to TiNTs, FLUM and FLUM@TiNTs showed electric signal fluctuation ranging from 5% (for control) up to 20% (for FLUM) until 120 min of the experiment. Furthermore the conductivity of this polarized membrane was studied *via* the modulation of the ion channels

at the end of the experiment (Fig. 6). The response of the membrane to the addition of forskolin or bumetanide, which modifies the voltage dependent K$^+$ of a healthy membrane, supports the lack of toxicity of both, TiNTs and FLUM@TiNTs. Indeed, the voltage dependent K$^+$ of intestine exposed to TiNTs or FLUM@TiNTs increased significantly compared to those of control or FLUM. In contrast, a slightly decrease of voltage dependent K$^+$ of intestine exposed to FLUM (compared to the control) was observed, probably indicating a membrane suffering.

Furthermore, the diffusion flux (F) and the apparent permeability of the membrane (P_{app}) for TiNTs, FLUM and FLUM@TiNTs were calculated (Fig. 7 and 8). Thanks to TiNTs a high value of FLUM diffusion flux regardless the intestine section were observed. Interestingly, TiNTs increased significantly the permeation flux of FLUM 12 folds compared to free FLUM. Likewise it is worth mentioning that high nanotubes concentrations (empty TiNTs or FLUM@TiNTs) are able to cross the intestine *via* enterocytes without inducing toxicity as evidenced by histological examination of intestine (Fig. 9).
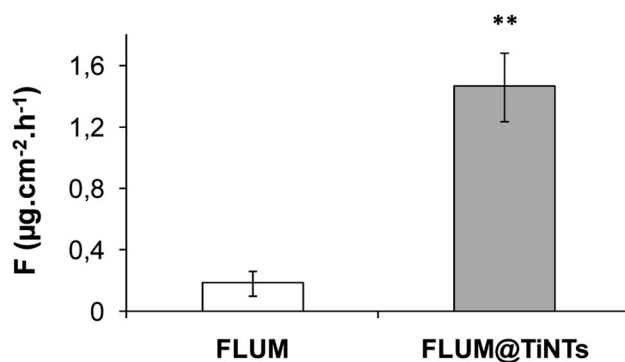

Fig. 7 Diffusion flux (F) of FLUM *versus* FLUM@TiNTs studied on sea bass intestine after 2 h of exposition in the Ussing permeation chamber to FLUM (8 μg mL^{-1}) and FLUM@TiNTs (100 μg mL^{-1}). The permeation flux of FLUM@TiNTs is significantly higher than free FLUM (12 folds, $p < 0.01$). Data represent the mean ± SEM of 6 experiments and statistical significance was determined by Tukey HSD test (*$p < 0.05$, **$p < 0.01$).
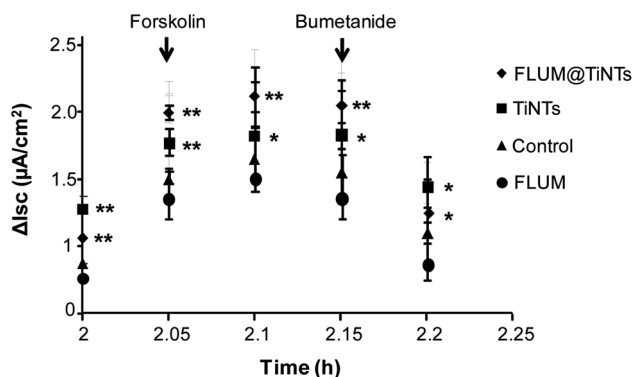

Fig. 6 Intestine membrane responses to the addition of forskolin (0.1 mM) or bumetanide (0.1 mM) after 2 h of membrane permeation studies with TiNTs, FLUM and FLUM@TiNTs at 37 °C compared to the control. Results are representative from six independent experiments (means ± SD, $n = 6$). Statistical significance (comparison with control or FLUM) was determined by Tukey HSD test (*$p < 0.05$, **$p < 0.01$).

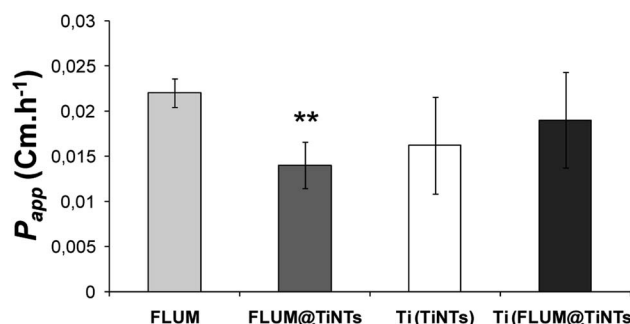**Fig. 8** Apparent permeability of the intestinal membrane (P_{app}) for TiNTs (100 μg mL^{-1}), FLUM (8 μg mL^{-1}) or FLUM@TiNTs (100 μg mL^{-1}) determined after 2 h of incubation at 37 °C in the Ussing chamber. Data represent the mean ± SEM of 6 experiments and statistical significance was determined by Tukey HSD test (**$p < 0.01$).
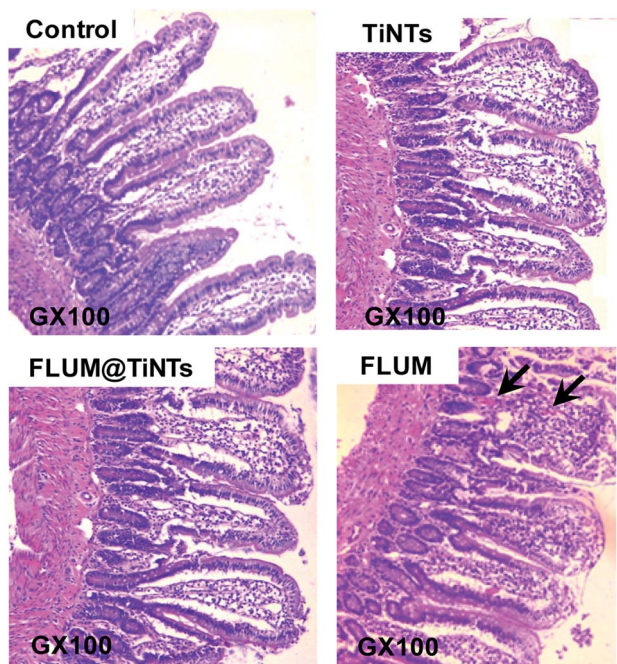
Fig. 9 Histological sections of sea bass intestine after 2 h of exposition in the Ussing permeation chamber to TiNTs (100 µg mL^{-1}), FLUM (8 µg mL^{-1}) and FLUM@TiNTs (100 µg mL^{-1}) compared with the control. Erosions with necrosis of the superficial part of the intestine mucosa (arrow) and enlargement of the villous axis are observed with FLUM exposition.

Indeed histological analysis of the intestine exposed to TiNTs revealed normal mucosa as compared with control characterized by a preserved architecture consisting of stender villi and glandular crypts well individualized. Contrary slightly histological damage including erosions with necrosis of the superficial part of the intestinal mucosa, enlargement of the villous axis and cellular desquamation and altered enterocytes were observed in the intestine exposed to FLUM (Fig. 8, arrows). The exposition to FLUM@TiNTs has protected the villous from the damage induced by free FLUM since normal villous relief and contour then well preserved intestine epithelia were observed without any histological lesions.

4 Discussion

In the current study, TiNTs were firstly tested for their stability in both ringer solution and M–H broth then for FLUM encapsulation and its release kinetic in PBS at 37 °C. Moreover FLUM@TiNTs was evaluated for its antibacterial activity against *E. coli* and its permeation across intestine of sea bass in the Ussing Chamber. The characterization shows that physicochemical properties of TiNTs are similar to those reported in the literature.[35,36] TiNTs shows a highly stability in both ringer solution and M–H broth as we have reported for DMEM and PBS solutions.[20] The stability is one of the most important parameters which can influence the release of the molecules loaded inside nanoparticles. Indeed, as the stability is high as the drug is protected and a sustained release is associated. This is

advantageous for titanium nanotubes compared to another biocompatible nanocarriers such as organic, inorganic and polymeric nanostructures, including dendrimers, micelles, and liposomes which are unstable in the biological medium.[16,37–39] In this regards TiNTs is progressively degraded only in acidic conditions (lysosome) as we have reported in our previous work.[22] In the encapsulation process ethanol solvent was used not only for its low toxic effect (rat oral LD$_{50}$ = 10.6 g kg^{-1}),[40] but also, for its high solubility of FLUM and its easy removal at low temperatures. Compared to FLUM nano-immobilized by self-assembly on iron oxide nanoparticles, the TiNTs encapsulation process is rapid and not costly since it plays a simple impregnation in ethanol and stirring. The mechanism of FLUM loading was based on the host–guest interactions mediated through TiNTs hydrogen bonds between FLUM molecules and nanotubes creating then a possible steric hindrance as reported previously.[41] Since high drug entrapment efficiency was achieved following 8 h of stirring, one can note that TiNTs pores presented affinity to guest alcohol rather than residual water within the multilayer nanotubes as described for other porous materials.[42,43] Moreover the geometrical properties of titanate nanotubes including longer tunable shape (80–1 µm) and small diameter (8–10 nm) play an important role in increasing the drug loading entrapment and prolonged release process.[44–46] Compared to carbon nanotubes,[47] or to spherical and hybrid nanomaterials[48–51] or to polymeric delivery systems of fluoroquinolones,[52] TiNTs shows a highly entrapment efficiency of FLUM with a perfect sustained release. The evaporation of solvents (ethanol and water), packed on the surface and in the interior of pores nanotubes, plays an important role in the retention of drug within the pores by forming crystalline grains which becomes bigger with the increasing of drug loading amount and stable by the intermolecular bonding forces as confirmed for other drug molecules within TiNTs.[53] The burst release of FLUM observed when starting the stirring of FLUM@TiNT in the PBS can be ascribed to the release of the adsorbed FLUM molecules on the TiNTs surface as a result of the high concentration gradient between the TiNTs and surrounding medium. In the same manner, it was reported that gentamicin molecules adsorbed on TiNTs nanotubes surface were rapidly released.[30] It is worthy to point that molecules charge is another factor affecting the drug release process. Indeed, FLUM loading bring positive charges to the empty nanotubes which are negatively charged thanks to the hydroxyl groups on the surface and within layers, thus causing a stronger ionic interaction. Consequently, the drug release occurs slower as has been described for TiNTs with other antibiotics.[54,55] Additionally, cation exchange of the alkyl amino groups of quinolones can play an important role in the adsorption mechanism of drug on nanomaterials surface by forming highly stable chemical bonds, causing a prolonged drug release as described for montmorillonite nanomaterials.[56,57] Concerning the antibacterial effect, no obvious difference in the viability of *E. coli* was observed between the control and TiNTs-treated bacteria, indicating the biocompatibility of the nonmaterials TiNTs as shown for several cells *in vitro*.[19,20] On the other hand, *E. coli* was strongly inhibited in the presence of free FLUM (8 µg

mL^{-1}) because of the high drug concentration which is 2 times higher than the minimum inhibitory concentration (MIC $\approx$ 4 μg mL^{-1} for *E. coli*).[58] However, after 3 days of incubation, a rebound effect of bacterial growth was occurred. The hypothesis of bacterial resistance is ruled out because the development of FLUM resistance usually needs much longer time of exposure (more than 150 days).[59,60] Thus, we suggest that the degradation of FLUM in the broth and/or its metabolization within bacterial cell are the principle causes of its low antibacterial activity as reported.[60,61] The treatment with FLUM@TiNTs induced a progressive damage and cells death indicating that TiNTs enhances the drug efficacy thanks to their protection mechanism from degradation and progressive release during the experiment period. Given the advantages of drug encapsulation which include (i) a sustained release that can reduce frequent doses administration and side effects, (ii) an enhanced absorption,[62] the use of TiNTs as FLUM nanocarrier appears as an attractive alternative for better FLUM release and antibacterial efficiency. Another point to be considered is that the tunable shape of this nanocarrier can facilitates the bacterial membrane passage inside cytoplasm improving thus its antibacterial activity as shown in our previous work on the interaction of genistein loading TiNTs with U87-MG cells.[20] Therefore, the strong antimicrobial activity owing to cell membrane damage resulted from direct contact of cells with aggregated FLUM@TiNTs as shown for carbon nanotubes agglomerated (SWCNTs) on outer semi permeable membrane of *E. coli* accompanied by more severe cellular damage.[63] Considering that the bacterial outer membrane drives the cell adhesion process through their highly charged structure and their functional groups such as carboxyl, hydroxyl, phosphate or amide,[64–66] we suggest that FLUM@TiNTs uptake mechanism by *E. coli* was mediated through a binding of nanotubes to the negatively charged bacterial membrane surface, prompting thus membrane damage.

Finally, the intestinal barrier bypass of TiNTs, FLUM, and FLUM@TiNTs, as well as their potential toxicity over the intestine were studied *ex vivo* using permeation Ussing chamber. Compared to the free antibiotic, TiNTs act to increase the intestinal permeation of FLUM during the experiment. Indeed the encapsulated FLUM flux and permeation increased in a like manner to those of TiNTs proving that antibiotic pass across the intestinal epithelium *via* nanotubes. Thanks to its physical properties (diameter 10 nm, tubular shape…) TiNTs are easy uptaken by enterocytes thus involving endocytosis mechanism as demonstrated in our previous work studying the internalization of TiNTs by U87MG cells *in vitro*.[20] Moreover small nanoparticles with diameter <50–100 nm are known to pass through enterocytes by endocytosis mechanism.[67] Thereby TiNTs improves intestinal permeation of FLUM 12 folds compared to the free antibiotic without inducing any toxicity. The safety of TiNTs was reported for mice after intravenous administration of a relatively high dose of 45 mg kg^{-1} during 45 days.[21] Moreover the use of large sized nanomaterials in drug delivery poses major problems, including *in vivo* instability, poor bioavailability, and poor solubility, poor absorption in the body, issues with target-specific delivery, and tonic

effectiveness, and probable adverse effects of drugs.[68,69] Interestingly, the high stability of TiNTs regardless of simulated physiological medium plays an important role in protecting antibiotic particularly against chelating with divalent ions including Ca^{2+} and Mg^{2+}. Indeed these ions are rich in marine environment and in fish feed; when they are associated to the fluoroquinolones they reduced significantly their intestinal absorption.[70] Various nanostructures, including liposomes, polymers, dendrimers, silicon or carbon materials, have been tested as carriers in drug delivery systems[39] but no one of them was tested for antibiotic delivery in aquaculture probably due to their instability in marine environment and incapacity to protect antibiotic against chelating with divalent ions. Further studies are needed to elucidate these points. Due to its high stability in the simulated intestinal medium, TiNTs are promising protections of the most sensitive intestinal microorganisms against the bactericidal effect of FLUM. Taken together, FLUM@TiNTs formulation paves the way for future pharmacokinetic studies of FLUM in the treatment of fish infections, and significantly reduces the excessive use of antibiotic which improve the survival in a healthy environment. Noteworthy, this sustained-release formulation can be also tested for other animals farming including pig and poultry.

5 Conclusion

TiNTs were tested for FLUM encapsulation and its release kinetic in PBS at 37 °C. Then the drug loaded nanotubes were evaluated for its antibacterial activity against *E. coli*, a fish pathogenic bacterium and its intestinal permeation in Ussing chamber. The geometrical properties of titanate nanotubes including longer tunable shape and small diameter play an important role in increasing the drug loading entrapment and a prolonged release up to 5 days. The strong antimicrobial activity owing to cell membrane damage resulted from the direct contact of cells with aggregated FLUM@TiNTs and the slow diffusion of FLUM inside bacteria. Interestingly a high chemical stability of TiNTs regardless of simulated physiological medium plays an important role in protecting antibiotic and improves its intestinal permeation 12 folds compared to the free antibiotic. Indeed FLUM pass across the intestinal epithelium *via* nanotubes which are internalized by enterocytes involving endocytosis mechanism. Taken together, FLUM@TiNTs formulation paves the way for future pharmacokinetic studies of FLUM in the treatment and targeting of fish infections, reducing the excessive use of antibiotic, and/or application for FLUM decontamination of polluted environment.

Author contributions

The manuscript was written through contributions of all authors. All authors have given approval to the final version of the manuscript.

Conflicts of interest

There are no conflicts to declare.

Acknowledgements

References

1 K. Tiseo, L. Huber, M. Gilbert, T. P. Robinson and T. P. Van Boeckel, *Antibiotics*, 2020, **9**, 918.

2 M. Pepi and S. Focardi, *Int. J. Environ. Res. Public Health*, 2021, **18**, 5723.

3 J. Kalantzi, A. Rico, K. Mylona, S. A. Pergantis and M. Tsapakis, *Sci. Total Environ.*, 2021, **764**, 142843.

4 H. Hektoen, J. A. Berge, V. Hormazabal and M. Yndestad, *Aquaculture*, 1995, **133**, 175–184.

5 M. Martinez, P. Mcdermontt and R. Walker, *Vet. J.*, 2006, **172**, 10–28.

6 D. Barrón, E. Jiménez-Lozano, S. Bailac and J. Barbosa, *Anal. Chim. Acta*, 2003, **477**, 21–27.

7 G. T. Haugland, K. O. Kverme, R. Hannisdal, M. Kallekleiv, D. J. Colquhoun, B. T. Lunestad, H. I. Wergeland and O. B. Samuelsen, *Front. Vet. Sci.*, 2019, **6**, 394–401.

8 M. O. Elema, K. A. Hoff and H. G. Kristensen, *Aquaculture*, 1995, **136**, 209–219.

9 B. Martinsen and T. E. Horsberg, *Antimicrob. Agents Chemother.*, 1995, **39**, 1059–1064.

10 O. B. Samuelsen and A. Ervik, *Aquaculture*, 1997, **158**, 215–227.

11 M. K. Hansen and T. E. Horsberg, *J. Vet. Pharmacol. Ther.*, 2000, **23**, 163–168.

12 M. O. Elema, K. A. Hoff and H. G. Kristensen, *Aquaculture*, 1994, **128**, 1–11.

13 L. Landgraf, I. Müller, P. Ernst, M. Schäfer, C. Rosman, I. Schick, O. Köhler, H. Oehring, V. V. Breus, T. Basché, C. Sönnichsen, W. Tremel and I. Hilger, *Beilstein J. Nanotechnol.*, 2015, **6**, 300–312.

14 M. Makowski, Í. C. Silva, C. Amaral, S. Q. Gonçalves and N. C. Santos, *Pharmaceutics*, 2019, **11**, 588–602.

15 K. P. Miller, L. Wang, B. C. Benicewicz and A. W. Decho, *Chem. Soc. Rev.*, 2015, **44**, 7787–7807.

16 J. K. Patra, G. Das, L. F. Fraceto, E. V. Campos, M. P. Rodriguez-Torres, L. S. Acosta-Torres, L. A. Diaz-Torres, R. Grillo, M. K. Swamy, S. Sharma, S. Habtemariam and H. S. Shin, *J. Nanobiotechnol.*, 2018, **16**, 7.

17 H. Zhang, Y. Sun, A. Tian, X. X. Xue, L. Wang, A. Alquhali and X. Bai, *Int. J. Nanomed.*, 2013, **8**, 4379–4389.

18 X. Niu, L. Sun, X. Zhang, Y. Sun and J. Wang, *Appl. Microbiol. Biotechnol.*, 2020, **104**, 2947–2955.

19 R. Moumita, C. Sriparna, D. Tanmay, B. Somnath, A. Pushan and M. Shyamalava, *Nanotechnology*, 2011, **22**, 5705–5718.

20 A. L. Papa, L. Dumont, D. Vandroux and N. Millot, *Nanotoxicology*, 2013, **7**, 11–31.

21 T. Baati, B. Kefi, A. Aouane, L. Njim, F. Chaspoul, V. Heresanu, A. Kerkeni, F. Neffati and M. Hammami, *RSC Adv.*, 2016, **6**, 101688.

22 T. Baati, L. Njim, S. Jaafoura, A. Aouane, F. Neffati, N. Ben Fradj, A. Kerkeni, M. Hammami and K. Hosni, *ACS Omega*, 2021, **6**(34), 21872–21883.

23 M. Bortolettia, S. Molinarib, L. Fasolatoa, J. Ugolottic, R. Tolosia, A. Venerandoa, G. Radaellia, D. Bertottoa, M. D. Liguoroa, G. Salviulob, R. Zborilc, F. Vianelloa and M. Magroa, *Colloids Surf., B*, 2020, **191**, 111019.

24 X. Lin, J. Li, S. Ma, G. Liu and K. Yang, *PLoS One*, 2014, **9**, 110247.

25 *Performance Standards for Antimicrobial Disk and Dilution Susceptibility Tests for Bacteria Isolated from Animals Approved Standard*, USA, 2nd edn, 2002.

26 *Methods for Broth Dilution Susceptibility Testing of Bacteria Isolated from Aquatic Animals*, Wayne, USA, 2006.

27 M. Roumi, E. Kwong, R. Deghenghi, V. Locatelli, S. Marleau, P. D. Souich, R. Beliveau and H. Ong, *Peptides*, 2001, **2**, 1129–1138.

28 *OECD Environment, Health and Safety Publications Series on Testing and Assessment*, Paris, 2006.

29 A. H. Bubolz, H. Li, Q. Wu and Y. Liu, *Am. J. Physiol.*, 2005, **289**, 1873–1880.

30 D. Krause, S. C. Lee and C. Deutsch, *Eur. J. Physiol.*, 1988, **412**, 133–140.

31 Y. Jiang, V. Ruta, J. Chen, A. Lee and R. Mackinnon, *Nature*, 2003, **423**, 42–48.

32 M. Touraki, M. Ladoukakis and C. Prokopiou, *J. Chromatogr. B: Biomed. Sci. Appl.*, 2001, **25**, 247–256.

33 S. Sahoo, C. K. Chakraborti and S. C. Mishra, *J. Adv. Pharm. Technol. Res.*, 2011, **2**, 195–204.

34 R. M. Silverstein, F. X. Webster, D. Kiemle and D. L. Bryce, *Spectrometric Identification of Organic Compounds*, John Wiley & Sons Edition, 2014.

35 S. Preda, V. S. Teodorescu, A. M. Musuc, C. Andronescu and M. Zaharescu, *J. Mater. Res.*, 2013, **28**, 294–303.

36 J. Nador, N. Orgovan, M. Fried, P. Petrik, A. Sulok, J. J. Ramsden, l. Korosi and R. Horvat, *Colloids Surf., B*, 2014, **122**, 491–497.

37 T. Baati, L. Njim, F. Neffati, A. Kerkeni, M. Bouttemi, R. Gref, M. F. Najjar, A. Zakhama, P. Couvreur, C. Serre and P. Horcajada, *Chem. Sci.*, 2013, **4**, 1597.

38 B. G. Esteban, L. C. Adolfo, H. C. Inocencio, V. F. Jesús and A. V. Alba, *Cancer Nanotechnol.*, 2019, **10**, 11.

39 L. Sercombe, T. Veerati, F. Moheimani, S. Y. Wu, A. K. Sood and S. Hua, *Front. Pharmacol.*, 2015, **6**, 286.

40 G. S. Wiberg, H. L. Trenholm and B. B. Coldwell, *Toxicol. Appl. Pharmacol.*, 1970, **16**, 718.

41 Y. Zhang, F. He, Z. Sun, L. Li and Y. Huang, *Mater. Lett.*, 2014, **128**, 384–387.

42 S. Devautour-Vinot, G. Maurin, F. Henn, C. Serre and G. Férey, *Phys. Chem. Chem. Phys.*, 2010, **12**, 12478.

43 S. Bourrelly, B. Moulin, A. Rivera, G. Maurin, S. Devautour-Vinot, C. Serre, T. Devic, P. Horcajada, A. Vimont, G. Clet, M. Daturi, J. C. Lavalley, S. Loera-Serna, R. Denoyel, P. L. Llewellyn and G. Férey, *J. Am. Chem. Soc.*, 2010, **132**, 9488.

44 k. N. Calıs, C. Bayram, E. Erdal, Z. Karahalilog and E. B. Denkbas, *Mater. Sci. Eng., C*, 2014, **35**, 100–105.

45 C. Moseke, J. M. Bae, S. Jin and S. Oh, *Appl. Surf. Sci.*, 2012, **258**, 5399–5404.

46 X. Xiao, L. Yang, M. Guo, C. Pan, Q. Cai and S. Yao, *Sci. China, Ser. B: Chem.*, 2009, **52**, 2161–2165.

47 S. B. Tiwari and M. M. Amiji, *Curr. Drug Delivery*, 2006, **3**, 219–232.

48 G. F. Paciotti, L. Meyer and D. Weinreich, *Drug Delivery*, 2004, **11**, 169–183.

49 D. Cunha, M. BenYahia, S. Hall, S. Miller, H. Chevreau, E. Elkaïm, G. Maurin, P. Horcajada and C. Serre, *Chem. Mater.*, 2013, **25**, 2767–2776.

50 D. H. Mobarak, S. Salah and S. A. Elkheshen, *Pharm. Dev. Technol.*, 2014, **19**, 891–900.

51 M. Salouti and A. Ahangari, *Nanoparticle Based Drug Delivery Systems for Treatment of Infectious Diseases*, InTech, New York, 2014.

52 K. Mulas, Z. Stefanowicz, E. Oledzka and M. Sobczak, *J. Controlled Release*, 2019, **294**, 195–215.

53 K. Gulati, K. Kant, D. Findlay and D. Losic, *J. Mater. Chem. B*, 2015, **3**, 2553–2559.

54 A. Hamlekhan, S. Sinha-Ray, C. Takoudis, M. T. Mathew, C. Sukotjo, A. L. Yarin and T. Shokuhfar, *J. Phys. D: Appl. Phys.*, 2015, **48**, 275401–275411.

55 K. C. Popat, M. Eltgroth, T. J. Latempa, C. A. Grimes and T. A. Desai, *Biomaterials*, 2007, **28**, 4880–4888.

56 Q. F. Wu, Z. Li, H. Hong, K. Yin and L. Tie, *Appl. Clay Sci.*, 2010, **50**, 204–211.

57 C. H. Wang, Z. Li, W. T. Jiang and J. S. Jean, *J. Hazard. Mater.*, 2010, **183**, 309–314.

58 J. Gomes, C. Lobo-Vilela, R. Bexiga, G. D. Nunes, N. Pereira and L. M. Cavaco, *Aquacult. Res.*, 2007, **38**, 613–617.

59 P. K. Hansen, B. T. Lunestad and B. Samuelsen, *Can. J. Microbiol.*, 1993, **39**, 1307–1312.

60 C. Concha, C. D. Miranda, L. Hurtado and J. Romero, *Microorganisms*, 2019, **7**, 698–714.

61 C. R. Da Silva, M. G. Maniero, S. Rath and J. R. Guimarães, *J. Adv. Oxid. Technol.*, 2011, **14**, 106–114.

62 F. Blasi, S. Aliberti and P. Tarsia, *Int. J. Nanomed.*, 2007, **2**, 551–559.

63 S. Liu, A. K. Keong, R. Xu, J. Wu, C. M. Tan, Y. Yang and Y. Chen, *Nanoscale*, 2010, **2**, 2744–2750.

64 W. Jiang, K. Yang, R. W. Vachet and B. Xing, *Langmuir*, 2010, **26**, 18071–18077.

65 A. Omoike and J. Chorover, *Biomacromolecules*, 2004, **5**, 1219–1230.

66 S. J. Parikh and J. Chorover, *Langmuir*, 2006, **22**, 8492–8500.

67 J. J. Powell, N. Faria, E. Thomas-McKay and L. C. Pele, *J. Autoimmun.*, 2010, **34**, 226–233.

68 N. Martinho, C. Damgé and C. P. Reis, *J. Biomater. Nanobiotechnol.*, 2011, **2**, 510.

69 H. Jahangirian, E. G. Lemraski, T. J. Webster, R. Rafee-Moghaddam and Y. Abdol-lahi, *Int. J. Nanomed.*, 2017, **12**, 2957.

70 S. C. Wallis, L. R. Gahan, B. G. Charles, T. W. Hambley and P. A. Duckworth, *J. Inorg. Biochem.*, 1996, **62**, 1–16.